Communications Earth & Environment https://doi.org/10.1038/s43247-026-03412-3

Article in Press

The world's enclosed seas highlight the need for urgent emission reductions and societal adaptation

Received: 11 November 2025

Accepted: 5 March 2026

Cite this article as: Gröger, M., Börgel, F., Dutheil, C. *et al.* The world's enclosed seas highlight the need for urgent emission reductions and societal adaptation. *Commun Earth Environ* (2026). https://doi.org/10.1038/s43247-026-03412-3

Matthias Gröger, Florian Börgel, Cyril Dutheil, Sven Karsten, H. E. Markus Meier, Kseniia Safonova & Georg Sebastian Völker

The world's enclosed seas highlight the need for urgent emission reductions and societal adaptation

Matthias Gröger[1], Florian Börgel[1], Cyril Dutheil[2], Sven Karsten[1], H.E. Markus Meier[1], Kseniia Safonova[1], Georg Sebastian Völker[1]

[1]Department of Physical Oceanography, Leibniz Institute for Baltic Sea Research Warnemünde, Seestraße 15, 181 19 Rostock, Germany

[2] MARBEC, University of Montpellier, CNRS, Ifremer, IRD, Sète, France, Montpellier

Corresponding author: Matthias Gröger, matthias.groeger@io-warnemuende.de

Abstract

Enclosed marginal seas are hotspots of endemic biodiversity that sustain societies through fisheries, tourism, and vital ecosystem services. Their small size makes them highly sensitive to global warming but systematic assessments of future climate change are lacking. Using climate model projections and reanalysis data, we assess two key thermal stressors across 19 seas: the rate of warming that limits the adaptive capacity of ecosystems, and the emergence of near-permanent marine heatwaves. We find these seas have already entered an unprecedented warming phase following the reversal of aerosol cooling effect in the late 20th century. Under unmitigated future scenarios, many seas would experience climate warming rates three to four times higher than previously observed, with 15 seas at risk of entering near-permanent heatwave states. Limiting global warming to below 2°C prevents such extremes, but seas still warm substantially: 13 seas exceed >1°C warming above preindustrial levels, and over 60% of the seas area transforms to a near-permanent heatwave state at mid-century. These findings highlight that even under the most optimistic scenarios, safeguarding the ecological integrity and socioeconomic value of marginal seas demands transformative adaptation, proactive conservation, and large-scale restoration efforts.

1. Introduction

Enclosed marginal seas (EMS) lie at the interface between land and open ocean and play a vital role for both ecosystems and societies. They contribute considerably to global food production through fisheries and aquaculture, offer key spaces for recreation and tourism, and can serve as important carbon sinks that help to meeting national and global emission targets. In addition, EMS provide a wide range of climate services, including coastal protection, biodiversity support, and vigorous primary production.

However, EMS are also among the most impacted marine regions worldwide, subject to overlapping pressures from coastal intervention, eutrophication, pollution, and overfishing, compounded by climate-driven stressors such as ocean warming and acidification. The combination of anthropogenic and climatic drivers makes EMS particularly vulnerable to rapid and potentially irreversible change. For example, nutrient input and contemporaneous marine heatwaves (MHW) can lead to deoxygenation in stratified EMS[1].

Ocean warming trends are of particular concern[2]. Rising temperatures directly alter the thermal habitats of marine organisms, posing serious threats to slow-adapting species such as benthic invertebrates, corals, and cold-water fish. Warming also drives an increase in the frequency, intensity, and duration of marine heatwaves (MHW), which can cause mass mortalities[3], coral bleaching[4,5], and large-scale ecosystem restructuring[6]. MHW have already emerged as one of the most acute threats to marine biodiversity and fisheries sustainability[7]. In EMS, basin-wide MHW are particularly likely, because of their small size and restricted water exchange with the open ocean. Such events are also more severe, as they affect the thermal refugia of entire ecosystems simultaneously[8,9]. As outlined by Amaya et al.[10] MHW definitions need a clear rationale to be useful for practical usage such as coastal management. We here

choose the approach of a fixed baseline derived from the undisturbed climate period 1850-1899. This approach particularly highlights changes that occurred already in the course of climate warming and may lead in extreme scenarios to the phenomenon of quasi-permanent MHW.

Despite their global importance and vulnerability, detailed climate projections are lacking for most marginal seas . While some regions—such as the Mediterranean[11], the Baltic Sea[12–15], the North Sea[16–19] , the Sea of Japan[20,21], or the Gulf of Mexico[22,23], are the subject of extensive ongoing research, many others lack the systematic, region-specific climate information urgently needed to support adaptation and management.

To address this gap, the present study provides a global assessment of warming trends and projected MHW emergence across 19 major marginal seas (Figure 1). By analyzing ensemble climate model projections under both high-emission and mitigated scenarios, we provide the first comprehensive picture of how EMS as a whole respond to future climate warming, including the risk of transitions into near-permanent heatwave states. This global perspective is essential for informing coordinated marine conservation strategies, international climate negotiations, and the sustainable management of coastal ocean resources in a warming World.

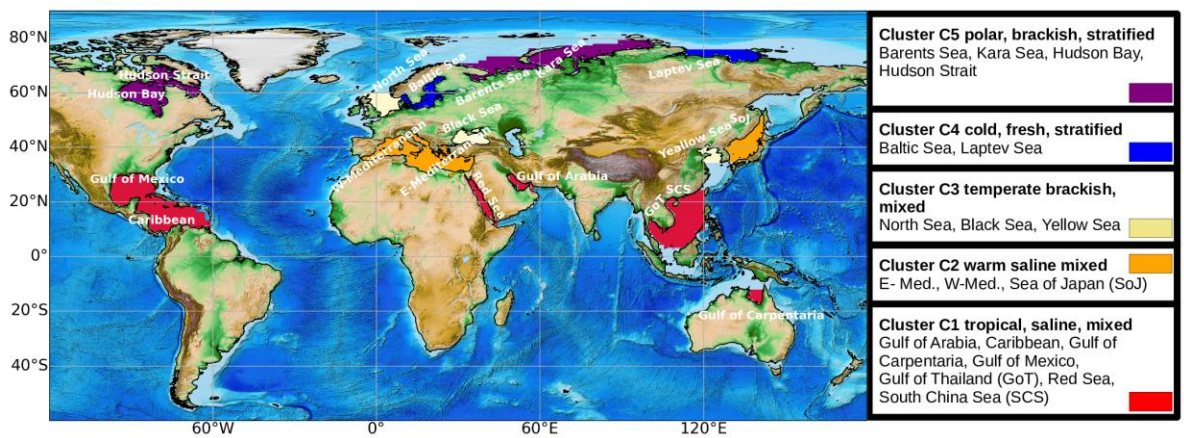

Figure 1: Nineteen enclosed marginal Seas investigated in this study. red = tropical-saline-mixed, blue = cold-fresh-stratified, purple = polar-brackish-stratified, orange = warm-saline-mixed, yellow = temperate-brackish-mixed. Categorization of EMS (right panel) is based on average sea surface temperature, salinity, and mixed layer depth (see methods section 2). Please note, the outer borders of individual EMS may deviate from other used definitions to avoid the inclusion of areas too far outside land enclosure. Note that many very small EMS could not considered in this study since they were not resolved in the model system.

2 Results

We use the Max Planck Institute Grand Ensemble[24] (MPI-GE), which is briefly described and validated in Supplementary. Figure. 1, and Supplementary Table1. It allows a robust separation of forced climate signals from internal variability, which is essential for estimating the probability of rare extremes in relatively small and variable systems such as EMS. While other Grand Ensembles from various modeling centers exist, the MPI-GE is one of the few that provides daily SST output. MPI-GE is unique among model ensembles because its climate sensitivity has

been tuned to the observed value for greenhouse gases[25]. As a result, it exhibits a climate sensitivity of ~2.8°C, which is close to the observational estimate of 3.0°C[24]. This makes it particularly well-suited for studying warming trends and marine heatwave (MHW) conditions. To further ensure accuracy, we trend-corrected the MPI-GE ensemble to align with observed warming since the satellite era. This correction preserves the model's internal variability and its projected future forced changes (see methods, section 1).

2.1 Global warming impact on EMS

To illustrate the results, the 19 EMS were partitioned into five physically coherent clusters using multivariate classification of SST, salinity, and mixed-layer depth (online methods section 2).

EMS exhibit larger internal variability than the open oceans making long term trends more difficult to detect. Nevertheless, long term observed SST data since 1950 show a clear positive SST trend since the end of the last century (Figure 2a). Notably, after ~2010, all EMS clusters except the tropical one warm faster than the global average (Figure 2a), a feature well captured by the MPI-GE (Figure 2b). In particular, the recent SST anomalies, for the temperate (C3), cold (C4) and polar (C5) EMS - clusters are twice as high compared to entire World ocean.

By averaging across the 50-member ensemble, we isolate the forced, anthropogenic warming signal from natural variability. This signal shows a pronounced acceleration, with decadal warming rates peaking around the year 2000 in all EMS (Figure 2c). These peaks were unprecedented in the historical record, where forced trends were dominated by the short cooling and warming cycles caused by volcanic aerosols (Figure 2d). Notably, this year-2000 warming boost is rarely reached again after 2000, even in the high-end SSP5-8.5 scenario (Figure 2c). The exception is the polar cluster, which shows higher trends in the second half of the 21st century—a finding consistent with the well-established phenomenon of polar amplification[26].

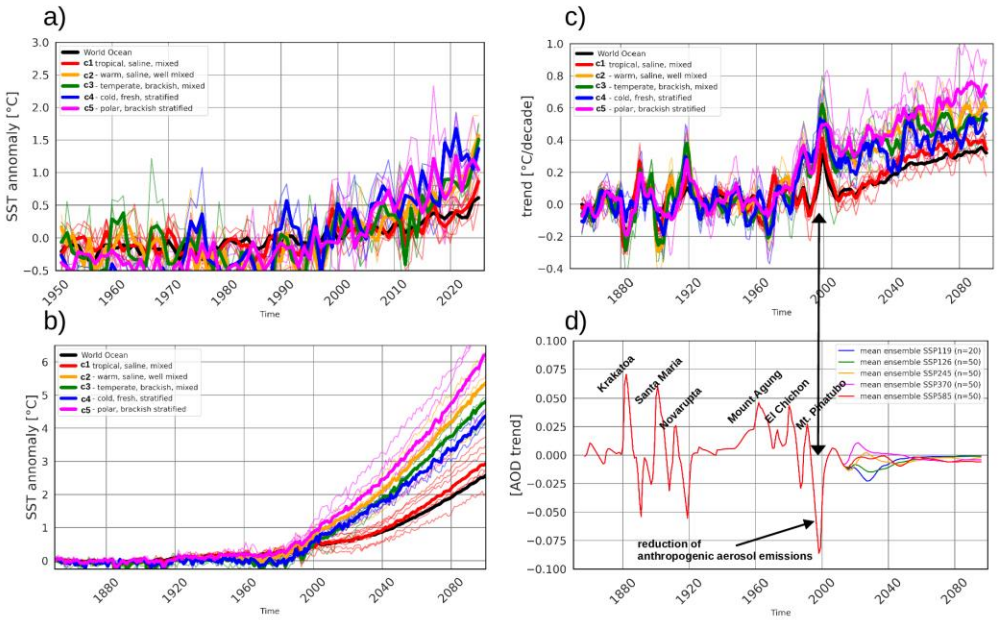

Figure 2: a) Annual EMS mean temperature anomalies relative to the mean temperature 1950 – 2024 based on the ERA5 reanalysis data set[53]*. b) Annual EMS mean SST anomalies relative to the mean temperature 1850 – 1899 following SSP5-8.5. c) EMS decadal SST trends under SSP5-8.5. Thick colored lines in a) – c) indicate EMS cluster averages of the same physical habitat depicted from the preindustrial era (methods section 1). Thick black line denotes global averages of the entire World Ocean for comparison. d) EMS decadal trends for atmospheric optical density for the historical period and the future according to SSPs. The arrow marks contemporaneous peak trends in AOD and decadal warming. All curves are based on ensemble averages.*

The sensitivity to climate warming is illustrated exemplary by the high-end GHG scenario SSP8.5 which represents a completely unmitigated scenario (Fossil-Fueled Development). Aligning the trends for the recent past, a total warming between +2°C and +7°C is reached at the end of the century (Figure 2b). Again all clusters are above the mean warming of the World ocean, highlighting the high sensitivity of EMS. The polar stratified cluster (C5) shows strongest warming and reaches a SST anomaly of >+6°C at the end of the 21st century. Cold, temperate, and warm EMS (i.e. clusters C4, C3, C2) warm between +4.0 and 5.5°C. Tropical EMS show least warming which on average only slightly warm more than the global average. However, the spread among EMS is fairly high in this cluster and so three EMS reach a warming >3°C.

The peak warming rates around 2000 correspond to a peak negative trend in the atmosphere's optical density over the respective EMS (Figure 2c,d) which suggests the accelerated warming is a direct effect of the gradual reduction of industrial aerosols in developed countries at the end of the 20th century[27]. The speed at which current warming occurs plays a crucial role, as it constrains the time window for marine life to adapt[2,28]. This raises an important question: *could future global warming lead to warming magnitudes in the World's EMS similar to or even greater than those observed in recent decades?*

To answer this, we must consider not just the magnitude of warming but also its relevance for the marine ecosystem. Since multi-decadal warming rates disproportionately threaten the richest areas of marine biodiversity[2,28], we include 30-year trends in our analysis alongside decadal ones. We consider two complementary metrics: (i) forced trends, defined as the 50-member ensemble mean capturing the systematic response to greenhouse gases, and (ii) discrete trends, which measure the probability of exceeding historical maxima after 2020 (see methods section 3). Together, these metrics capture both the anthropogenic signal and the stochastic variability of the climate system. We define excess trends (ETs) as those after 2020 that exceed the maximum trends observed before 2020.

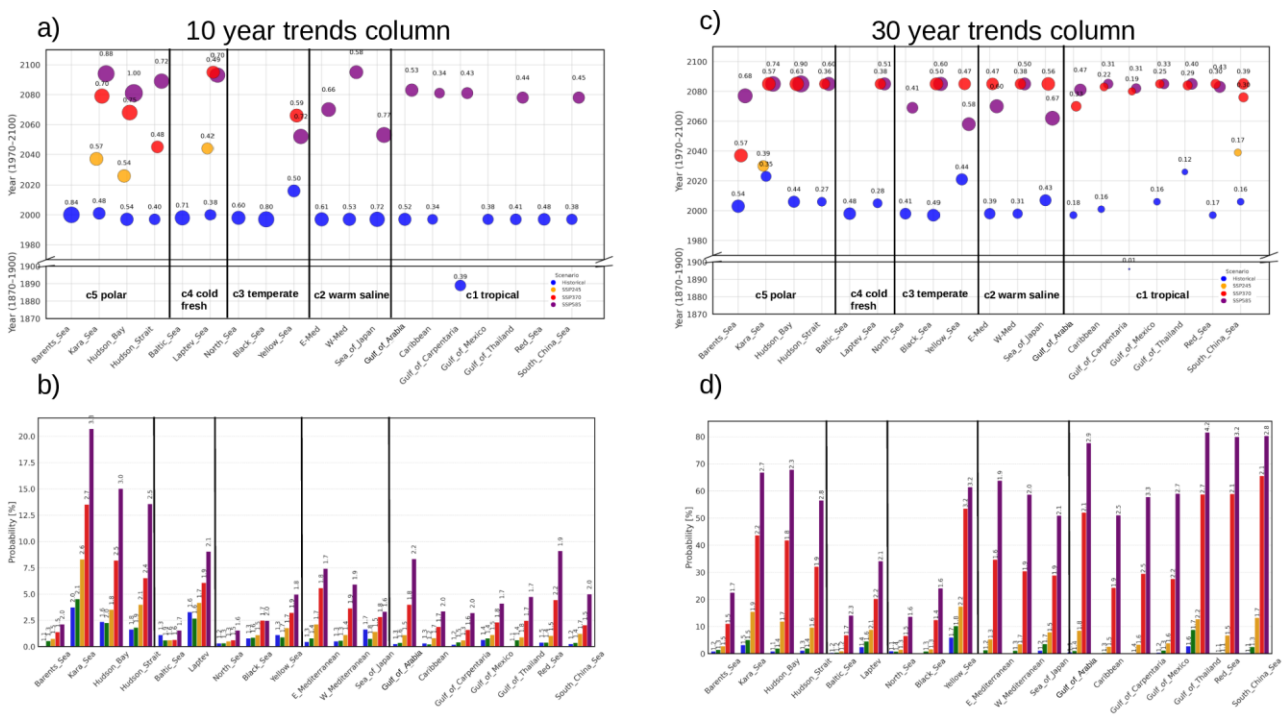

Figure 3: Trend analysis for 19 enclosed marginal seas considered in this study. a) Forced (=ensemble mean) maximum decadal warming trends [°C/decade] depicted from the historical period and projected trends for higher emission SSP scenarios. Blue symbols indicate the maximum for the historical period until 2020. For the future after 2020, only trends are indicated which exceed those in the historical period. b) Probability for respective EMS to experience higher warming trends after 2020 than before 2020 (see methods section 3). Number on top of the bars denote the biggest trends found after 2020 expressed as ratio maxtrend_after 2020/maxtrend_before_2020. Hence, a value of 2.2 for SSP5-8.5 for the Gulf of Arabia means the highest 10-year trend diagnosed after 2020 exceeds the highest trend before 2020 by a factor of 2.2. c) same as a) but maximum trends over 30-year periods are considered. d) same as b) but for 30-year-trends. Vertical lines separate physical habitat clusters.

The scenarios SSP3-7.0 and SSP5-8.5 bear an extraordinary high risk for forced ETs (Figure 3a,c). SSP2-4.5 demonstrates already a substantial mitigation as only three (10-year trends) or two (30-year trends) EMS would experience ETs (all of them belonging to the cold-fresh or polar cluster).

The Paris compliant SSP1-1.9 and SSP1-2.6 forced trends define the safe space that avoids ETs completely. Notably, for decadal trends (Figure 3a), 6 EMS never reach their historical maxima even under the high-end SSP5-8.5 scenario, highlighting the big 20th century warming boost in these regions. An exception is the Gulf of Carpentaria, where the largest trends occur in the late nineteenth century, likely triggered by the nearby Krakatoa eruption 1883.

Located in the southern hemisphere north of Australia, this sea was sheltered from the major anthropogenic aerosol sources during the 20th century.

Figure 3b,d addresses the discrete risk to face ETs in future. In case of decadal trends this risk is fairly low with only three sea-ice bearing EMS having a >10% probability reaching ETs within this century. On the other hand, due to the strong climate variability on decadal time scales, even in the SSP1-1.9, reflecting a +1.5°C World, a risk for ETs remains, but this risk is in all EMS lower than 4%.

By contrast, the 30-year trends, in which short term variability is damped, respond more to (GHG-)forced trends and thus, the risk for ETs is overall higher reaching >80 % in certain seas in SSP3-7.0 and SSP5-8.5 (Figure 3d). In these EMS warming trends 3 to 4 times higher than ever before emerge (e.g. Red Sea, Gulf of Thailand, Figure 3d). Overall, the lowest risk for ETs is projected for European EMS such as the Baltic Sea or North Sea, mainly because of extraordinary high historical trends associated with the cleaning atmosphere over Europe around 2000[29].

2.2 Climate impact on marine heatwaves

We apply the concept of seasonally varying temperature thresholds to identify marine heatwave (MHW) events, following the definition of Hobday et al.[30] and employing a fixed-baseline approach. In this framework, daily and spatially varying thresholds are calculated from historical simulations for the period 1850–1899. As a result, the probability of exceeding these fixed thresholds increases with ongoing climate warming, which may lead to the emergence of permanent MHW conditions under strong warming scenarios, thereby losing their episodic nature[10]. This approach was chosen to emphasize changes relative to the undisturbed preindustrial climate and to assess under which scenarios, and at what time, permanent MHW conditions may arise.

The accelerated warming observed in recent decades has already increased the global risk of MHW by roughly threefold since 2000[31]. For EMS, this intensification raises the likelihood to transit into a permanent and basin-wide MHW state, because of their limited size and restricted water exchange. However, our analysis revealed that fully permanent basin-wide MHW states are nevertheless virtually impossible, since short-term interruptions caused by atmospheric variability and transient weather systems periodically break the persistence of extreme temperatures. We therefore focus on the likelihood of EMS reaching a *near-permanent* MHW state—defined as periods when the annual average MHW extent exceeds 90% of the total EMS area and the number of MHW days surpasses 330 (90% of all days in a year). Two key events were focused:

1. First: the year in which a basin-wide MHW is first detected.
2. near-Permanent. the year in which a near-permanent MHW state is established.

Together these events can inform whether the “first time” events could serve as an early warning signal for near-permanent MHW in the respective EMS. Both these events are influenced by the forced mean warming rate, as well

as by the stochastic uncertainty associated with natural variability. As such, the results are presented as probability distributions, as shown in Figure 4.

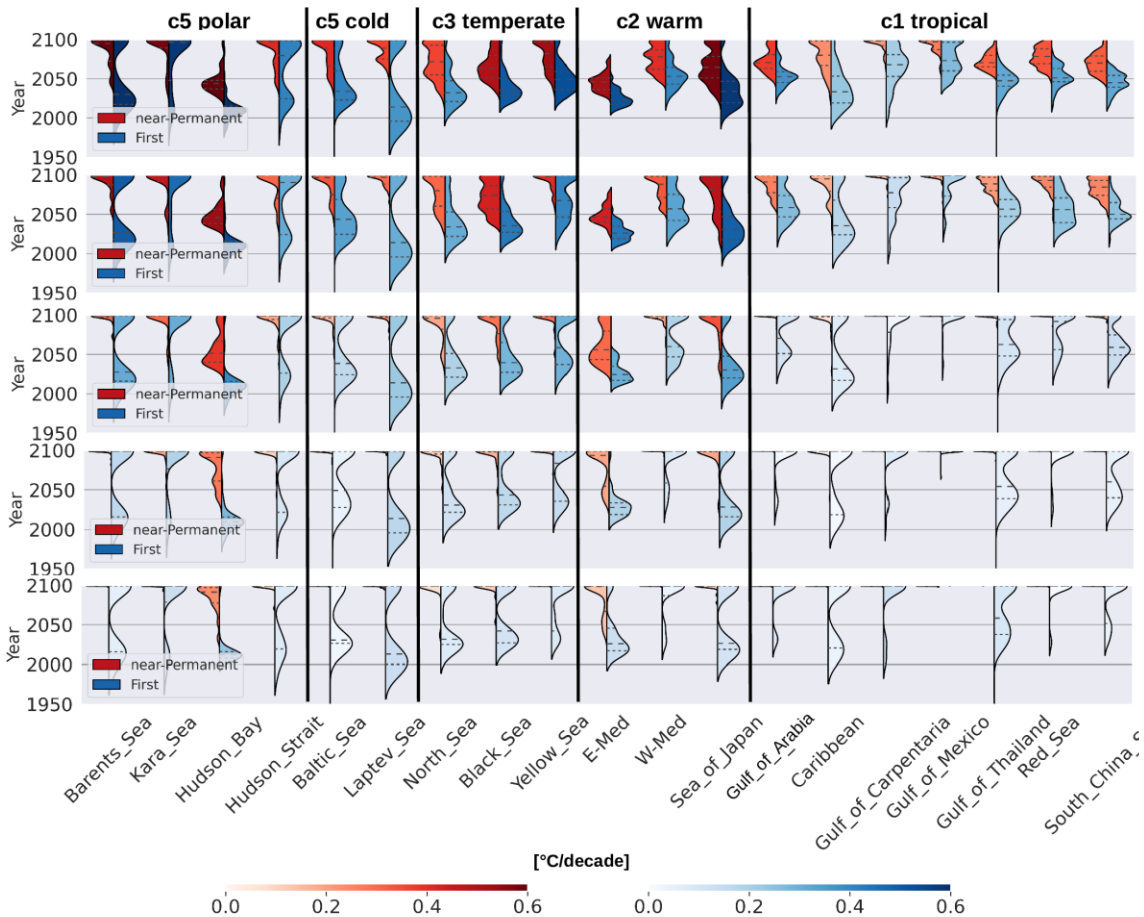

Figure 4: Probabilistic evaluation of marine heatwave events.Violin-plot displaying probability density distributions using a kernel density estimator. blue = year of first occurrence of a basin wide MHW. red: year entering a quasi-near permanent MHW, i.e. the year when the yearly average MHW extent remains permanently >90% of the total basin area and the yearly number of MHW days is permanently >90% of the total days within a year. Dashed horizontal line within the violins denote the median and inter-quartile range. The dimension-less width of the violins is determined by the number of observations within each `basin` *category. The blue and red color bars denote the forced warming trend averaged over the 50 member ensemble for each respective EMS and SSP scenario. Note, the forced mean trends for "first" and "permanent" are identical, but red and blue colors are chosen to better distinguish the respective probability distributions. Also note, the calculations for SSP1-1.9 are based on only 20 instead of 50 ensemble members which induces higher statistical uncertainties. This may lead for example to the counterintuitive fact of greater forced trends in this scenario than in higher SSPs (as the case for e.g. the Gulf of Thailand). MHW were detected using the method of Hobday et al., (2016) relative to thepreindustrial baseline 1850-1899 (see methods section 4).*

2.2.1 First basin-wide events

The First events of a basin-wide MHW show a notable spread over time in most EMS, suggesting that such event is largely driven by internal variability. Consequently, the first occurrence cannot be considered a reliable early indicator for the onset of a permanent MHW state in the near future. Overall, the likelihood to register a “first” event within the first hundred years after the onset of industrialization (1850-1950) is extremely low but increases substantially thereafter. With higher SSP scenarios, the temporal overlap between the "first" and "near-permanent" distributions reduces and the spread over time shortens. In these cases, MHW trends are mainly driven by the stronger forced warming trends. Consequently, the time interval between the "first" and "permanent" MHW can be expected shorter in these higher emissions scenarios.

2.2.2 Near-permanent MHW

The likelihood for a certain EMS to reach a quasi-permanent MHW state clearly scales with the magnitude of the forced warming trend (indicated by the color scale of the violins in Figure 4) and thus depends largely on the SSP scenario (Figure 4). In the majority of EMS, permanent MHW states can be safely avoided in SSP1-1.9/SSP1-2.6 (exceptions: Hudson Bay and Eastern Mediterranean).

Based on the probability density distributions (Figure 4), we derived quantiles to classify the likelihood of each EMS transitioning into a near-permanent marine heatwave (MHW) state as highly likely (≥80% probability), likely (≥50%), or of low likelihood (≥20%, Supplementary Table 3). Under the high-emission scenario SSP5-8.5, a near-permanent MHW state is highly likely in 12 EMS and likely in 18 EMS by the end of the century. In contrast, under the low-emission scenario SSP1-2.6, only two EMS exhibit a ≥50% probability of such a transition. These findings highlight the effectiveness of the Paris goals in significantly reducing the risk of near-permanent MHW conditions.

2.3 Climate mitigation effect of the Paris 2015 targets

Even if the Paris climate targets successfully mitigate future warming rates, the EMS will continue to warm, reaching SST anomalies on average of 1.5°C (SSP1-1.9) or 1.8°C (SSP1-2.6) by mid-century (Figure 5a). The EMS would then stabilize at a level ~0.7°C lower than under the moderate SSP2-4.5 scenario, where SSTs keep rising beyond 2100.

However, marine heatwaves (MHW) will remain a serious threat even if global warming is stabilized within the Paris targets. Under the SSP1-1.9 scenario, over 60% of the total EMS area will be subject to MHW conditions (Figure 5b). Similarly, the risk of basin-wide MHW events will persist (Figure 4) even though they do not indicate an imminent transition to a near-permanent MHW state.

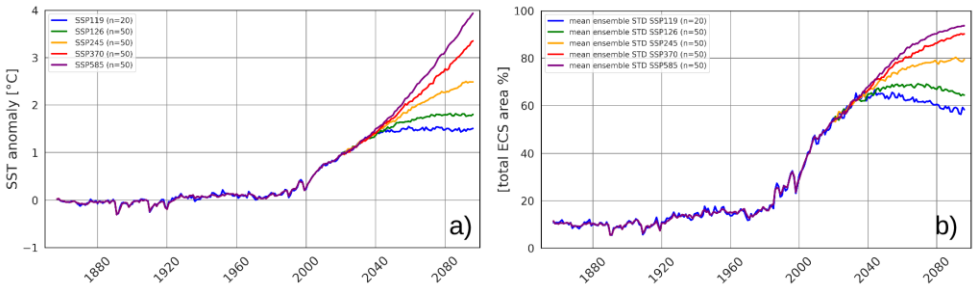

Figure 5: Mitigation effect according to potential future SSPs. a) Sea surface temperature anomalies averaged over the entire EMS area compared to the pre-industrial era. b) Annual average fraction of MHW area of total EMS area. Averages over all EMS and all ensemble members are shown.

To provide a detailed mitigation-assessment, we ranked the EMS based on six key thermal stressors, classifying them into six severity categories under a mitigated global warming scenario of +2°C (SSP1-2.6, methods section 5). Overall, the resulting ranking aligns with the physical habitat clusters (Figure 6). Polar and sub-polar basins (e.g., Hudson Bay, Barents Sea, Kara Sea, Laptev Sea) dominate the high-severity end, identifying them as hotspots for rapid MHW intensification and geographic expansion.

Tropical basins (e.g. Caribbean, Gulf of Arabia, Gulf of Carpentaria, Gulf of Mexico) align predominantly at the low-severity end, with low warming trends and weak MHW intensity increases. Most other EMS (e.g. Mediterranean, Baltic, Yellow Sea, North Sea) fall in between, showing regionally elevated risks but not consistently across all indicators. Notably, all EMS but two are likely to reach a state where ≥50% of the respective EMS area is occupied by a MHW in the yearly average at the end of the 21st century.

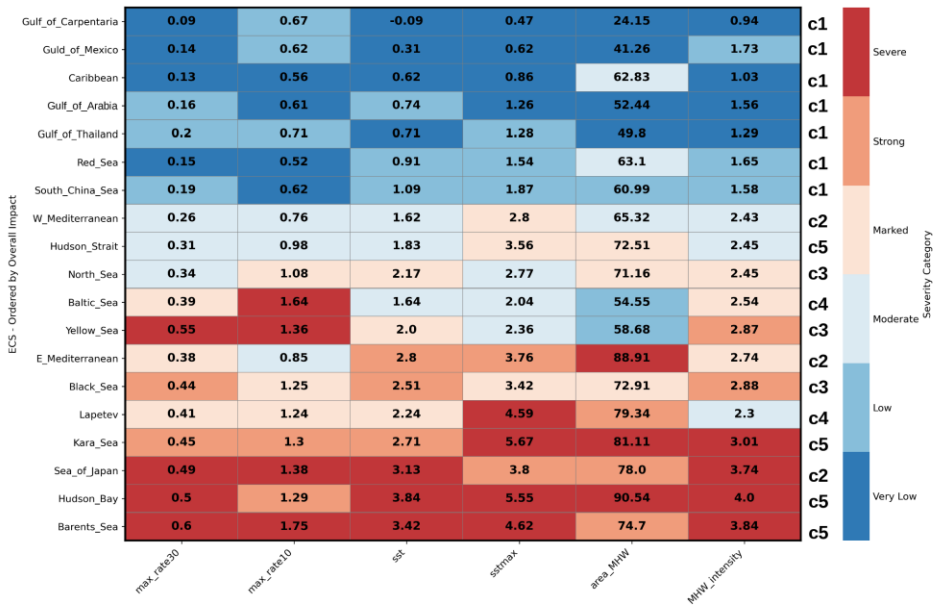

Figure 6: Climate impact map for 6 key indicators of climate change in EMS based on SSP1-2.6. max_rate30 and max_rate10 denote the maximum detected 30-year period and 10-year period forced trend after 2020. sst and sstmax denote the increase of yearly mean SST [°C] and mean annual maximum SST [°C] for 2080 -2099 compared to the preindustrial era. area_mhw denotes the yearly average MHW area fraction [%] in 2080 – 2099 compared to the preindustrial era. MHW_intensity denotes the of average sst anomalies reached during MHW in 2080 – 2099 compared to the preindustrial era. The cluster the individual EMS belong to, are indicated between the map and the color scale. The ranking is based on normalized evaluation summarizing all 6 indictors (methods section 5)

Discussion

This study identified a concerted warming spike across most EMS in the late 20th century. Accelerated by cleaning air conditions[27] this spike was unprecedented since the onset of industrialization. This underscores that the world's EMS have already entered a phase of exceptional thermal stress, manifested in the occurrence of devastating MHW worldwide[4,12,32,33]. These accelerated warming trends have already produced major ecological impacts across various EMS: shifts in species distributions[34], population declines[33], changes in community structures[35], reduced biodiversity[2], and losses of ecosystem services such as fisheries[33,36] productivity[17,37] and carbon sequestration[38–40].

We demonstrate that the Paris compliant scenarios of maximal 1.5 or 2.0 °C global warming (SSP1-1.9 and SSP1-2.6), mark the safe space for EMS. Under these pathways the probability for unprecedented warming rates reduces to less than 10% (Figure 3b,d) and near-permanent MHW are avoided. However, even this successful mitigation will likely not preserve EMS in their present ecological state. Under <2 °C of global warming, 13 out of 19 marginal seas will still warm between 1°C to ~3.5°C compared to pre-industrial levels (Figure 6). This committed warming leads to a persistent rise in MHW, resulting in 60% of the total marginal seas area being permanently under their influence. For seven marginal seas, there is at least a 20% likelihood of transitioning to a near-permanent MHW state within this century (Supplementary . Table 3). Hence, such transition implies the need for strategies to cope

particularly with long lasting extreme water temperatures in addition to develop strategies to mitigate short term periods of extensive warming which is important to distinguish as outlined by Amaya et al.[10]

Consequently, many EMS will undergo considerable structural and functional changes, including shifts in species composition, productivity, and habitat suitability. Therefore, while climate mitigation is non-negotiable for preventing the most extreme outcomes, it must be complemented by robust adaptation and restoration strategies to build resilience against unavoidable thermal stress. Given the inevitability of these changes, we recommend a strategic shift in research resources toward developing early prediction systems for MHW[41] and transform themse tools into operational services for marine planning agencies. We note however, that many of todays interventions, show limited capacity to buffer marine ecosystems against warming[42] in particular for tropical coral reef systems[43]. Hence, more targeted actions that alleviate other local stressors in parallel such as water-quality improvements may be more successful[44].

By contrast, under high-end scenarios (SSP3-7.0 and SSP5-8.5) the overall warming becomes so pronounced that the probability to exceed unprecedented 30-year warming rates rises by up to 80% (Figure 3,d). Because simulations end in 2099, these extreme rates could only be tracked until 2085, yet it is likely that they persist and further increase well into the 22nd century. Such high warming rates over this long time would drive species redistribution beyond current endemic ranges, with rates of redistribution higher than ever before[2]. Paleoclimate evidence suggests that rates consistent with SSP2-4.5 would endanger up to 70% of today's richest regions of marine biodiversity[2].

Of course, future warming will act alongside other climate-related stressors not investigated in this study. Consequently, compound events of MHW, hypoxia, and ocean acidity extremes[38,45] will become more likely and more disruptive in future, thereby leaving potentially irreversible effects on the regional ecosystem structure. Due to their land enclosure, EMS particularly prone to multiple, often compound environmental and anthropogenic stressors. Yet, the role of compound events has only occasionally gained recognition, primarily in well monitored EMS like the Baltic Sea where climate change emerged as significant as all current pressures combined[46,47]. Warming winters combined with MHW and prevailing fishing pressure have driven severe declines in herring and cod population[33,36] which are the economically most important fish stocks in the Baltic Sea.

The found overall lower temperature changes in tropical EMS does not necessarily indicate a lower pressure to such marine ecosystems. This is because many tropical species already live near their upper thermal tolerances so that even small increases in thermal stress could have a large negative effect[48] while species from temperated mid-latitude regions often have higher tolerances[48,49].

Some unavoidable limitations are associated with this study. The coarse resolution of the global model ensemble limits its ability to capture local (sub-basin) characteristics and to resolve very small but important EMS which could not be included in this study (such as the e.g. Chesapeake Bay). To translate our findings into actionable recommendations for adaptation and management, more systematic assessments with high-resolution regional

models are needed. Such targeted studies would allow the development of locally adapted strategies that smartly account for the specific oceanographic and ecological characteristics of respective EMS. Uncertainty with respect to the choice of the model system could not be assessed since only a small minority of available model centers provide such such huge ensembles with daily SST output. Among these few model systems, MPI-GE was selected because its climate sensitivity is closest to observations.

Acknowledgments

The research presented in this study is part of the Baltic Earth program (Earth System Science for the Baltic Sea region; see www.baltic.Earth) and a contribution to the BMBF funded project CoastalFutures (03F0911E). We thank the Max Planck Institute for Meteorology for providing the MPI-GE.

Author Contributions

M.G. designed the study, performed the analysis and wrote the text. CD, MM, SK, GV, KS, FB contributed with comments about scientific content/analysis, read and approved the manuscript.

Methods

Section 1: Trend bias correction

An accurate representation of temperature trends is a key benchmark for evaluating climate models, and is often more relevant than absolute climatological biases[50]. This is because trend fidelity reflects the model's response to external forcings, such as those defined by the Radiative Concentration Pathways (RCPs). The ability to reproduce observed trends is strongly influenced by a model's climate sensitivity, typically quantified as Transient Climate Response (TCR).

To account for systematic biases in simulated trends, we applied a trend correction to the sea surface temperature (SST) fields from MPI-GE prior to analysis, as follows:

1. Compute linear SST regressions for each of the 50 MPI-GE ensemble members at every grid cell over the historical period 1980–2014.

$$\beta_i^{\mathrm{MPI}}(x,y) = \mathrm{linreg}_{t\in\mathcal{T}}\left(T_i^{\mathrm{MPI}}(x,y,t)\right)$$

with T_i^{MPI} the SST(x,y) and x,y =lon,lat at time t and i_l[50] the ensemble member

2. Repeat the same trend calculation for ERA5 SST data over the same period and grid.

$$\beta^{\mathrm{ERA5}}(x,y) = \mathrm{linreg}_{t\in\mathcal{T}}\left(T^{\mathrm{ERA5}}(x,y,t)\right)$$

<

3. Determine the trend bias by subtracting the MPI-GE trend (ensemble mean or individual members) from the ERA5 trend at each grid point.

$$\Delta\beta_i(x,y) = \beta^{\mathrm{ERA5}}(x,y) - \beta_i^{\mathrm{MPI}}(x,y)$$

4. Apply the correction by adding these trend differences to the original SST time series of each MPI-GE ensemble member.

$$T_i^{\mathrm{corr}}(x,y,t) = T_i^{\mathrm{MPI}}(x,y,t) + \Delta\beta_i(x,y)\cdot(t-t_0)$$

The picture below exemplary shows the SST results of the correction for a grid cell located in the North Sea at 0.8°E; 57.8°N (central north Sea): Green original time series; black corrected time series.

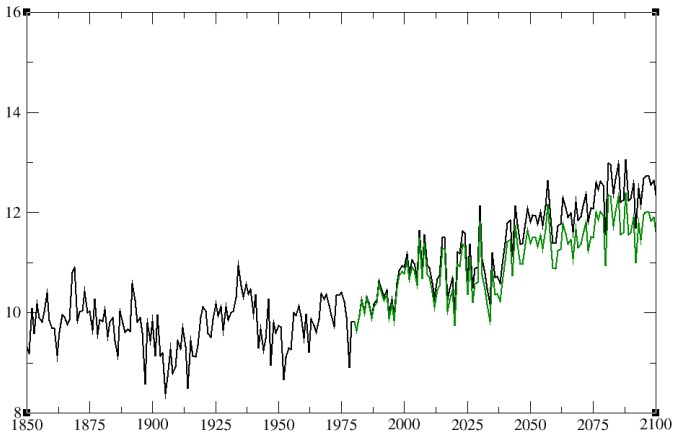

Section 2: EMS Categorization based to their physical habitat

The World's EMS span a highly diverse range of marine ecosystem services, habitats for marine life, geomorphology, and economic usage. However, a systematic categorization of the World's EMS including all aspects environmental and human indicators is still lacking, and far beyond the scope of current study. We here build upon the concept of "Large Marine Ecosystems" (LMEs) which is funded on 5 criteria modules: productivity, fish and fisheries, pollution and ecosystem health, socioeconomics, and governance resulting in 64 different LMEs. We adapt this concept but further categorize LMEs by main oceanographic properties, i.e. SST, salinity, and mixed layer depth that are available from the CMP6 archive. These properties are employed to determine similar physical habitats that directly influence marine ecosystems by controlling nutrient availability, stratification, oxygen levels, species distribution, and ultimately marine productivity.

We employed multivariate classification methods to identify EMS clusters that share similar environmental characteristics and climate sensitivities. The grouping of EMS was performed by k-means clustering — an unsupervised machine learning technique — to group data into distinct clusters based on similarity. The assignment to the clusters is determined by an algorithm that iteratively minimizes euclidean distances to the clusters centroids. The algorithm then assigns data points to the nearest cluster. The optimal number of clusters for each analysis was determined beforehand using the silhouette and elbow method. The analysis was performed using the python package scikit-learn[51] from which further details of the method can be obtained. The results are shown in Figure 7.

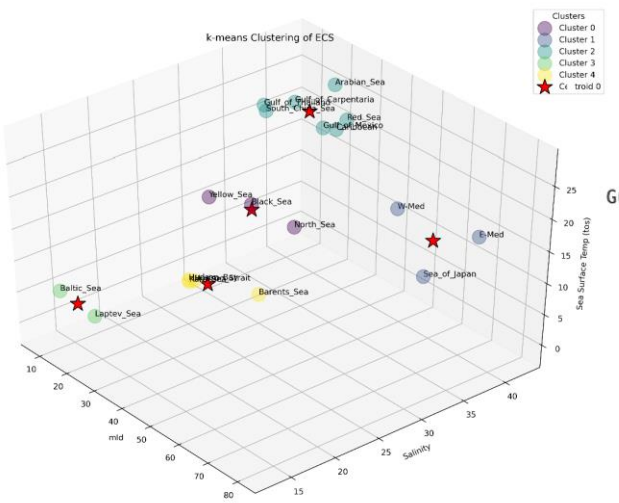

basin	cluster
Gulf_of_Arabia	1
Caribbean	1
Gulf_of_Carpentaria	1
Gulf_of_Mexico	1
Gulf_of_Thailand	1
Red_Sea	1
South_China_Sea	1
E-Med	2
Sea_of_Japan	2
W-Med	2

basin	cluster
Black_Sea	3
North_Sea	3
Yellow_Sea	3
Baltic_Sea	4
Laptev_Sea	4
Barents_Sea	5
Hudson_Bay	5
Hudson_Strait	5
Kara_Sea	5

Figure 7: Results of k-means clustering. Colored circles indicate the position of individual seas in the parameter space (mixed layer, salinity, sea surface temperature). Red stars indicate the position of the 5 cluster centroids. Cluster assignment for each sea is given in the text box.

Finally, using the clusters centroids, the found clusters are assigned to characteristic physical marine habitats:

Habitat assignment of EMS clusters based on physical properties				
cluster	**mld [m]**	**salinity [g/kg]**	**SST [°C]**	**physical habitat**
C1	29.60	36.06	26.59	tropical, saline, mixed
C2	70.77	36.07	17.23	warm, saline well mixed
C3	24.73	31.03	12.90	temperate, brackish, mixed
C4	10.25	15.50	2.50	cold fresh, stratified
C5	17.08	28.28	0.3	polar, brackish, stratified

We note the resulting clusters largely reflect the existing concept of large marine Ecosystems (LME). However in most cases LMEs encompass a quite large extent towards the open sea which we would like to avoid for the current studies concept of (land-)enclosed marginal seas.

Section 3. Probability Analysis for 30-year trends

We assessed the occurrence of strong decadal warming trends in sea surface temperature (SST) time series derived from the MPI-GE. The method is illustrated exemplary for trends over 30 years and was likewise done for 10-year periods in an analog way. The analysis was performed using the climate data operators (CDO) package and is described for the SSP1-2.6 scenario and across 50 ensemble members for each EMS. Other SSP are processed analogously.

30-year Trend Estimation

For each EMS basin B and ensemble member R

$$B \in \{1,2,3,\ldots,19\},\ R \in \{1,2,3,\ldots,50\}$$

we computed linear SST trends over moving 30-year windows, starting from the year 1850 through 2070. That is, for each starting year t, the trend $T_{B,R}(t)$ was estimated over the interval $[t,t+30]$.

We assumed that SST values Y_t over time follow a linear Gaussian model:

$Y_t = a+bt+\varepsilon_t,\ \varepsilon_t \sim N(0,\sigma^2)$

where a is the intercept, b is the linear trend (slope), and ε_t is normally distributed random noise. Following this assumption, the slope b was estimated using least-squares regression as:

$$T_{B,R}(t) = 10 \cdot \frac{\mathrm{Cov}(t,Y)}{\mathrm{Var}(t)} \qquad (1)$$

Here, Cov(t,Y) and Var(t) denote the covariance between time and SST and the variance of the time variable, respectively. The factor 10 rescales the linear trend to units of °C per decade.

Reference Trend Threshold

To define a threshold for strong warming trends, we identified, for each basin and ensemble member, the maximum decadal trend during the historical reference period 1850–2020:

$$T_{B,R}^{\max} = \max_{t \in \{1850,\ldots,2020\}} T_{B,R}(t) \qquad (2)$$

This threshold was used to detect anomalously strong trends in the future projection period.

Event Detection

We defined a **trend event** as any future 30-year period (centered from 2020–2085) during which the decadal SST trend equals or exceeds the historical maximum:

$$E_{B,R}(t) = \begin{cases} 1 & \text{if } T_{B,R}(t) \geq T_{B,R}^{\max} \text{ and } T_{B,R}(t) \neq \text{NaN} \\ 0 & \text{otherwise} \end{cases} \quad (3)$$

The number of detected events for each ensemble member was then given by:

$$N_{B,R} = \sum_{t=2020}^{2085} E_{B,R}(t) \quad (4)$$

This summation spans all possible 30-year windows between 2020 and 2085, resulting in a maximum of 66 detection opportunities per ensemble.

Ensemble Statistics and Probabilities

For each basin, we computed the mean number of events per ensemble:

$$\bar{N}_B = \frac{1}{50} \sum_{R=1}^{50} N_{B,R} \quad (5)$$

the probability of an event, is defined as the fraction of event-positive windows across all ensemble members:

$$P_B = \frac{1}{3300} \sum_{R=1}^{50} N_{B,R} = \frac{50 \cdot \bar{N}_B}{3300} \quad (6)$$

where 3300 is the total number of evaluated 30-year windows (66 per member × 50 members). This yields a basin-specific probability that a future 30-year window will exhibit a warming trend stronger than any observed in the historical baseline.

Section 4: Marine heatwave detection

Marine heatwaves (MHWs) are defined and categorized following Hobday[30]. According to this definition, an MHW event occurs when daily sea surface temperatures exceed the 90th percentile (PCTL90, hereafter) of a climatological baseline for 5 or more consecutive days. Short interruptions of up to two days below the threshold are tolerated within a single event.

MHW intensity is further categorized based on multiples of the difference between the daily PCTL90 and the multiyear average of daily mean temperatures over the reference period.

For future projections, MHWs are detected based on fixed thresholds derived from the pre-industrial reference climatology. This approach preserves the ability to assess total heat exposure on marine ecosystems under climate change, consistent with the rationale of Sen Gupta[52].

For each grid cell the following MHW indices were computed:

1. MHW frequency: the number of MHW events per year.

2. MHW duration: Average duration of individual MHW events within a 30-year period.

3. MHW days: Total number of MHW days per year, averaged over the 30-year period.

4. MHW extent: Yearly average spatial extent of MHWs across the entire EMS.

In this study, two distinct reference periods were used for the calculation of marine heatwave (MHW) metrics, depending on the objective of the analysis.

To assess the response to climate change, the reference climatology was derived from the last 330 years of the pre-industrial control simulation. For each calendar day of the year, the threshold calculations (e.g., PCTL90) are thus based on 330 values, providing a statistically robust estimate of daily climatological extremes.

For the validation of the MPI-ESM model, however, we relied on observed sea surface temperatures (SSTs) from the ERA5 reanalysis product, for which no pre-industrial data are available. Consequently, the reference period for validation was set to 1982–2014. The upper bound of 2014 aligns with the end of the historical simulation period in the CMIP6 framework, while the lower bound (1982) was selected due to the increased reliability of SST observations from that year onward, coinciding with the assimilation of satellite-based measurements. This results in

only 33 years of data available per calendar day, which poses a challenge for estimating higher percentiles like the 90th percentile (PCTL90), due to insufficient sample size.

To address this limitation, and following the recommendation of Hobday[30], we applied an 11-day moving window centered on each calendar day. This approach increases the effective sample size to 363 values per day (11 × 33), enhancing the statistical robustness of the calculated daily thresholds for MHW detection during the validation period.

Section 5: Composite Impact Ranking

To assess and rank the relative severity of climate change indicators across basins, we constructed a composite performance score based on the normalized values of six key indicators. These include

- $x_1 = \text{max\_rate30}$ max warming trend over 30-year periods
- $x_2 = \text{max\_rate10}$ max warming trend over 10-year periods
- $x_3 = \text{sst}$ increase in area averaged yearly mean SST in 2080 – 2099 compared to 1850 – 1999
- $x_4 = \text{sstmax}$ area averaged yearly maximum SST in 2080 – 2099 above the 1850 – 1999 state
- $x_5 = \text{area\_MHW}$ yearly average MHW area fraction
- $x_6 = \text{MHW\_intensity}$ mean sst anomaly reached during MHWs

1. Normalization

Each indicator x_j was min-max normalized to the range [0,1] across all basins to ensure comparability:

$$x'_{i,j} = \frac{x_{i,j} - \min(x_j)}{\max(x_j) - \min(x_j)} \quad (1)$$

where:

$x_{i,j}$ is the value of indicator j for basin i,

$x'_{i,j}$is the normalized value,

$\min(x_j)$ and $\max(x_j)$ are the minimum and maximum values of indicator *j* across all basins.

This transformation ensures that $x'_{i,j} \in [0,1]$, where 0 corresponds to the least severe value (lowest impact), and 1 to the most severe (highest impact).

2. Composite score

A composite performance score S_i was then calculated for each basin ii as the unweighted arithmetic mean of its normalized indicators:

$$S_i = \frac{1}{6}\sum_{j=1}^{6} x'_{i,j} \quad (2)$$

This score reflects the average relative severity of marine heatwave conditions in each basin, with lower scores indicating lower impact.

3: Ranking

Basins were then ranked in ascending order of S_i with rank 1 assigned to the basin with the lowest composite score (lowest impact), and the highest rank assigned to the basin with the highest impact score.

Data availability statement

This study uses output from the MPI Grand Ensemble (MPI-GE) generated with the Max Planck Institute for Meteorology Earth System Model. The data are distributed through the Earth System Grid Federation (ESGF) and can be accessed via the Deutsches Klimarechenzentrum ESGF node (project: mpi-ge, https://esgf-data.dkrz.de). Users must register with ESGF and agree to the CC BY-SA 4.0 license prior to download. Data source files to reproduce the figures are available under https://doi.org/10.5281/zenodo.18723187.

Competing interests

The authors declare no competing interests.

References

1. Safonova, K., Meier, H. E. M. & Gröger, M. Summer heatwaves on the Baltic Sea seabed contribute to oxygen deficiency in shallow areas. *Commun Earth Environ* **5**, 106 (2024) https://doi.org/10.1038/s43247-024-01268-z.
2. Brown, S. C., Mellin, C., García Molinos, J., Lorenzen, E. D. & Fordham, D. A. Faster ocean warming threatens richest areas of marine biodiversity. *Global Change Biology* **28**, 5849–5858 (2022) https://doi.org/10.1111/gcb.16328.
3. Garrabou, J. *et al.* Marine heatwaves drive recurrent mass mortalities in the Mediterranean Sea. *Global Change Biology* **28**, 5708–5725 (2022) https://doi.org/10.1111/gcb.16301.
4. Dutheil, C. *et al.* The massive 2016 marine heatwave in the Southwest Pacific: An "El Niño–Madden-Julian Oscillation" compound event. *Sci. Adv.* **10**, eadp2948 (2024) https://doi.org/10.1126/sciadv.adp2948.
5. Frölicher, T. L. & Laufkötter, C. Emerging risks from marine heat waves. *Nat Commun* **9**, 650 (2018) https://doi.org/10.1038/s41467-018-03163-6.
6. Stuart-Smith, R. D., Brown, C. J., Ceccarelli, D. M. & Edgar, G. J. Ecosystem restructuring along the Great Barrier Reef following mass coral bleaching. *Nature* **560**, 92–96 (2018) https://doi.org/10.1038/s41586-018-0359-9.
7. Holbrook, N. J. *et al.* Keeping pace with marine heatwaves. *Nat Rev Earth Environ* **1**, 482–493 (2020) https://doi.org/10.1038/s43017-020-0068-4.
8. Asner, G. P. *et al.* Mapped coral mortality and refugia in an archipelago-scale marine heat wave. *Proc. Natl. Acad. Sci. U.S.A.* **119**, e2123331119 (2022) https://doi.org/10.1073/pnas.2123331119.
9. Minobe, S. Exceptional heat and basin-scale connections in the Kuroshio–Oyashio region in the early 2020s. *J Oceanogr* **81**, 443–461 (2025) https://doi.org/10.1007/s10872-025-00764-w.
10. Amaya, D. J. *et al.* Marine heatwaves need clear definitions so coastal communities can adapt. *Nature* **616**, 29–32 (2023) https://doi.org/10.1038/d41586-023-00924-2.
11. Soto-Navarro, J. *et al.* Evolution of Mediterranean Sea water properties under climate change scenarios in the Med-CORDEX ensemble. *Clim Dyn* **54**, 2135–2165 (2020) https://doi.org/10.1007/s00382-019-05105-4.
12. Meier, H. E. M. *et al.* Oceanographic regional climate projections for the Baltic Sea until 2100. *Earth Syst. Dynam.* **13**, 159–199 (2022) https://doi.org/10.5194/esd-13-159-2022.

13. Dutheil, C., Meier, H. E. M., Gröger, M. & Börgel, F. Understanding past and future sea surface temperature trends in the Baltic Sea. *Clim Dyn* **58**, 3021–3039 (2022) https://doi.org/10.1007/s00382-021-06084-1.

14. Gröger, M., Arneborg, L., Dieterich, C., Höglund, A. & Meier, H. E. M. Summer hydrographic changes in the Baltic Sea, Kattegat and Skagerrak projected in an ensemble of climate scenarios downscaled with a coupled regional ocean–sea ice–atmosphere model. *Clim Dyn* **53**, 5945–5966 (2019) https://doi.org/10.1007/s00382-019-04908-9.

15. Dutheil, C., Meier, H. E. M., Gröger, M. & Börgel, F. Warming of Baltic Sea water masses since 1850. *Clim Dyn* **61**, 1311–1331 (2023) https://doi.org/10.1007/s00382-022-06628-z.

16. Tinker, J. *et al.* Twenty-first century marine climate projections for the NW European shelf seas based on a perturbed parameter ensemble. *Ocean Sci.* **20**, 835–885 (2024) https://doi.org/10.5194/os-20-835-2024.

17. Gröger, M., Maier-Reimer, E., Mikolajewicz, U., Moll, A. & Sein, D. NW European shelf under climate warming: implications for open ocean – shelf exchange, primary production, and carbon absorption. *Biogeosciences* **10**, 3767–3792 (2013) https://doi.org/10.5194/bg-10-3767-2013.

18. Mathis, M. & Pohlmann, T. Projection of physical conditions in the North Sea for the 21st century. *Clim. Res.* **61**, 1–17 (2014) https://doi.org/10.3354/cr01232.

19. Schrum, C. *et al.* Projected Change—North Sea. in *North Sea Region Climate Change Assessment* (eds Quante, M. & Colijn, F.) 175–217 (Springer International Publishing, Cham, 2016). doi:10.1007/978-3-319-39745-0_6 https://doi.org/10.1007/978-3-319-39745-0_6.

20. Deegala, D. & Chung, E.-S. Future projection of marine heatwaves in a global marine hotspot: case of East/Japan sea. *Clim Dyn* **63**, 194 (2025) https://doi.org/10.1007/s00382-025-07682-z.

21. Sato, H. *et al.* Impact of an unprecedented marine heatwave on extremely hot summer over Northern Japan in 2023. *Sci Rep* **14**, 16100 (2024) https://doi.org/10.1038/s41598-024-65291-y.

22. Chollett, I., Müller-Karger, F. E., Heron, S. F., Skirving, W. & Mumby, P. J. Seasonal and spatial heterogeneity of recent sea surface temperature trends in the Caribbean Sea and southeast Gulf of Mexico. *Marine Pollution Bulletin* **64**, 956–965 (2012) https://doi.org/10.1016/j.marpolbul.2012.02.016.

23. Bove, C. B., Mudge, L. & Bruno, J. F. A century of warming on Caribbean reefs. *PLOS Clim* **1**, e0000002 (2022) https://doi.org/10.1371/journal.pclm.0000002.

24. Olonscheck, D. *et al.* The New Max Planck Institute Grand Ensemble With CMIP6 Forcing and High-Frequency Model Output. *J Adv Model Earth Syst* **15**, e2023MS003790 (2023) https://doi.org/10.1029/2023MS003790.

25. Mauritsen, T. *et al.* Developments in the MPI-M Earth System Model version 1.2 (MPI-ESM1.2) and Its Response to Increasing CO_2. *J Adv Model Earth Syst* **11**, 998–1038 (2019) https://doi.org/10.1029/2018MS001400.

26. Rantanen, M. *et al.* The Arctic has warmed nearly four times faster than the globe since 1979. *Commun Earth Environ* **3**, 168 (2022) https://doi.org/10.1038/s43247-022-00498-3.

27. Quaas, J. *et al.* Robust evidence for reversal of the trend in aerosol effective climate forcing. *Atmos. Chem. Phys.* **22**, 12221–12239 (2022) https://doi.org/10.5194/acp-22-12221-2022.

28. Beaty, F., Gehman, A. M., Brownlee, G. & Harley, C. D. G. Not just range limits: Warming rate and thermal sensitivity shape climate change vulnerability in a species range center. *Ecology* **104**, e4183 (2023) https://doi.org/10.1002/ecy.4183.

29. Wild, M., Wacker, S., Yang, S. & Sanchez-Lorenzo, A. Evidence for Clear-Sky Dimming and Brightening in Central Europe. *Geophysical Research Letters* **48**, e2020GL092216 (2021) https://doi.org/10.1029/2020GL092216.

30. Hobday, A. J. *et al.* A hierarchical approach to defining marine heatwaves. *Progress in Oceanography* **141**, 227–238 (2016) https://doi.org/10.1016/j.pocean.2015.12.014.

31. Marcos, M., Amores, A., Agulles, M., Robson, J. & Feng, X. Global warming drives a threefold increase in persistence and 1 ° C rise in intensity of marine heatwaves. *Proc. Natl. Acad. Sci. U.S.A.* **122**, (2025) https://doi.org/10.1073/pnas.2413505122.

32. Holbrook, N. J. *et al.* A global assessment of marine heatwaves and their drivers. *Nat Commun* **10**, 2624 (2019) https://doi.org/10.1038/s41467-019-10206-z.

33. Gröger, M. *et al.* Future climate change and marine heatwaves - Projected impact on key habitats for herring reproduction. *Science of The Total Environment* **951**, 175756 (2024) https://doi.org/10.1016/j.scitotenv.2024.175756.

34. Calvet, N., Bluhm, B. A., Yoccoz, N. G. & Altenburger, A. Shifting invertebrate distributions in the Barents Sea since pre-1900. *Front. Mar. Sci.* **11**, 1421475 (2024) https://doi.org/10.3389/fmars.2024.1421475.

35. Berglund, Å. M. M. *et al.* Effects on the food-web structure and bioaccumulation patterns of organic contaminants in a climate-altered Bothnian Sea mesocosms. *Front. Mar. Sci.* **10**, 1244434 (2023) https://doi.org/10.3389/fmars.2023.1244434.

36. Möllmann, C. *et al.* Tipping point realized in cod fishery. *Sci Rep* **11**, 14259 (2021) https://doi.org/10.1038/s41598-021-93843-z.

37. Wabnitz, C. C. C. *et al.* Climate change impacts on marine biodiversity, fisheries and society in the Arabian Gulf. *PLoS ONE* **13**, e0194537 (2018) https://doi.org/10.1371/journal.pone.0194537.

38. Bindoff, N., Cheung, W. W. L. & Kairo, J. G. Changing Ocean, Marine Ecosystems, and Dependent Communities. in *The Ocean and Cryosphere in a Changing Climate* 447–588 (Cambridge University Press, 2022). doi:10.1017/9781009157964.007 https://doi.org/10.1017/9781009157964.007.

39. Hassoun, A. E. R. *et al.* Climate change risks on key open marine and coastal mediterranean ecosystems. *Sci Rep* **15**, 24907 (2025) https://doi.org/10.1038/s41598-025-07858-x.

40. Intergovernmental Panel On Climate Change (Ipcc). *Climate Change 2022 – Impacts, Adaptation and Vulnerability: Working Group II Contribution to the Sixth Assessment Report of the Intergovernmental Panel on Climate Change*. (Cambridge University Press, 2023). doi:10.1017/9781009325844 https://doi.org/10.1017/9781009325844.

41. Jacox, M. G. *et al.* Global seasonal forecasts of marine heatwaves. *Nature* **604**, 486–490 (2022) https://doi.org/10.1038/s41586-022-04573-9.

42. Danovaro, R. *et al.* Assessing the success of marine ecosystem restoration using meta-analysis. *Nat Commun* **16**, 3062 (2025) https://doi.org/10.1038/s41467-025-57254-2.

43. Bruno, J. F., Côté, I. M. & Toth, L. T. Climate Change, Coral Loss, and the Curious Case of the Parrotfish Paradigm: Why Don't Marine Protected Areas Improve Reef Resilience? *Annu. Rev. Mar. Sci.* **11**, 307–334 (2019) https://doi.org/10.1146/annurev-marine-010318-095300.

44. Donovan, M. K. *et al.* Local conditions magnify coral loss after marine heatwaves. *Science* **372**, 977–980 (2021) https://doi.org/10.1126/science.abd9464.

45. Burger, F. A., Terhaar, J. & Frölicher, T. L. Compound marine heatwaves and ocean acidity extremes. *Nat Commun* **13**, 4722 (2022) https://doi.org/10.1038/s41467-022-32120-7.

46. Wåhlström, I. *et al.* Projected climate change impact on a coastal sea—As significant as all current pressures combined. *Global Change Biology* **28**, 5310–5319 (2022) https://doi.org/10.1111/gcb.16312.

47. Wåhlström, I. *et al.* Combined climate change and nutrient load impacts on future habitats and eutrophication indicators in a eutrophic coastal sea. *Limnology & Oceanography* **65**, 2170–2187 (2020) https://doi.org/10.1002/lno.11446.

48. Vinagre, C. *et al.* Vulnerability to climate warming and acclimation capacity of tropical and temperate coastal organisms. *Ecological Indicators* **62**, 317–327 (2016) https://doi.org/10.1016/j.ecolind.2015.11.010.

49. Sunday, J. M., Bates, A. E. & Dulvy, N. K. Global analysis of thermal tolerance and latitude in ectotherms. *Proc. R. Soc. B.* **278**, 1823–1830 (2011) https://doi.org/10.1098/rspb.2010.1295.

50. Notz, D. How well must climate models agree with observations? *Phil. Trans. R. Soc. A.* **373**, 20140164 (2015) https://doi.org/10.1098/rsta.2014.0164.

51. Pedregosa, F. *et al.* Scikit-learn: Machine Learning in Python. *Journal of Machine Learning Research* **12**, 2825–2830 (2011).

52. Sen Gupta, A. Marine heatwaves: definition duel heats up. *Nature* **617**, 465–465 (2023) https://doi.org/10.1038/d41586-023-01619-4.

53. Bell, B. *et al.* The ERA5 global reanalysis: Preliminary extension to 1950. *Quart J Royal Meteoro Soc* **147**, 4186–4227 (2021) https://doi.org/10.1002/qj.4174.

Figure captions

Figure 1: Title: Nineteen enclosed marginal Seas investigated in this study.

red = tropical-saline-mixed, blue = cold-fresh-stratified, purple = polar-brackish-stratified, orange = warm-saline-mixed, yellow = temperate-brackish-mixed. Categorization of enclosed marginal sea (right panel) is based on average sea surface temperature, salinity, and mixed layer depth (see methods section 2). Please note, the outer borders of individual EMS may deviate from other used definitions to avoid the inclusion of areas too far outside land enclosure. Note that many very small EMS could not considered in this study since they were not resolved in the model system.

Figure 2: Analysis of climate change across 19 enclosed marginal seas

a) Annual EMS mean temperature anomalies relative to the mean temperature 1950 – 2024 based on the ERA5 reanalysis data set53. b) Annual EMS mean SST anomalies relative to the mean temperature 1850 – 1899 following SSP5-8.5. c) EMS decadal SST trends under SSP5-8.5. Thick colored lines in a) – c) indicate EMS cluster averages of the same physical habitat depicted from the preindustrial era (methods section 1). Thick black line denotes global averages of the entire World Ocean for comparison. d) EMS decadal trends for atmospheric optical density for the historical period and the future according to SSPs. The arrow marks contemporaneous peak trends in AOD and decadal warming. All curves are based on ensemble averages.

Figure 3: Title: Trend analysis for 19 enclosed marginal seas considered in this study.

a) Forced (=ensemble mean) maximum decadal warming trends [°C/decade] depicted from the historical period and projected trends for higher emission SSP scenarios. Blue symbols indicate the maximum for the historical period until 2020. For the future after 2020, only trends are indicated which exceed those in the historical period. b) Probability for respective EMS to experience higher warming trends after 2020 than before 2020 (see methods section 3). Number on top of the bars denote the biggest trends found after 2020 expressed as ratio maxtrend_after 2020/maxtrend_before_2020. Hence, a value of 2.2 for SSP5-8.5 for the Gulf of Arabia means the highest 10-year trend diagnosed after 2020 exceeds the highest trend before 2020 by a factor of 2.2. c) same as a) but maximum trends over 30-year periods are considered. d) same as b) but for 30-year-trends. Vertical lines separate physical habitat clusters.

Figure 4: Title: Probabilistic evaluation of marine heatwave events.

Violin-plot displaying probability density distributions using a kernel density estimator. blue = year of first occurrence of a basin wide MHW. red: year entering a quasi-near permanent MHW, i.e. the year when the yearly average MHW extent remains permanently >90% of the total basin area and the yearly number of MHW days is permanently >90% of the total days within a year. Dashed horizontal line within the violins denote the median and inter-quartile range. The dimension-less width of the violins is determined by the number of observations within each basin category. The blue and red color bars denote the forced warming trend averaged over the 50 member ensemble for each respective EMS and SSP scenario. Note, the forced mean trends for "first" and "permanent" are identical, but red and blue colors are chosen to better distinguish the respective probability distributions. Also note, the calculations for SSP1-1.9 are based on only 20 instead of 50 ensemble members which induces higher statistical uncertainties. This may lead for example to the counterintuitive fact of greater forced trends in this scenario than in higher SSPs (as the case for e.g. the Gulf of Thailand). MHW were detected using the method of Hobday et al., (2016) relative to thepreindustrial baseline 1850-1899 (see methods section 4).

Figure 5: Title: Mitigation effect according to potential future Shared Socioeconomic Pathways.

Mitigation effect according to potential future Shared Socioeconomic Pathways. a) Sea surface temperature anomalies averaged over the entire EMS area compared to the pre-industrial era. b) Annual average fraction of MHW area of total EMS area. Averages over all EMS and all ensemble members are shown.

Figure 6: Title: Climate impact of mitigation scenario SSP1-2.6

Climate impact map for 6 key indicators of climate change in EMS based on SSP1-2.6. max_rate30 and max_rate10 denote the maximum detected 30-year period and 10-year period forced trend after 2020. sst and sstmax denote the increase of yearly mean SST [°C] and mean annual maximum SST [°C] for 2080 -2099 compared to the preindustrial era. area_mhw denotes the yearly average MHW area fraction [%] in 2080 – 2099 compared to the preindustrial era. MHW_intensity denotes the of average sst anomalies reached during MHW in 2080 – 2099 compared to the preindustrial era. The cluster the individual EMS belong to, are indicated between the map and the color scale. The ranking is based on normalized evaluation summarizing all 6 indictors (methods section 5)

Editor's Summary:

Under 2 °C of mean global warming, 60% of the area of the world's enclosed marginal seas will be in a near-permanent marine heatwave state by the mid-century, according to a study employing climate model projections and reanalysis data.

Peer review information:

Communications Earth & Environment thanks Phillip Williamson and the other, anonymous, reviewer(s) for their contribution to the peer review of this work. Primary Handling Editors: Olusegun Dada and Alice Drinkwater. A peer review file is available.